Journal of Research and Applications in Mechanical Engineering
ISSN: 2229-2152 (Print); 2697-424x (Online)
(2020) Vol. 8, No. 2, 92-100
DOI: 10.14456/jrame.2020.11

Research Article

EFFECT OF BIODIESEL ON COMPRESSION IGNITION ENGINE'S COMBUSTION BEHAVIOR AND PARTICLE EMISSION

A. Tripatara[1]
P. Karin[1,*]
W. Phairote[1]
C. Charoenphonphanich[1]
M. Masomtob[2]
N. Chollacoop[2]
H. Kosaka[3]
[1] *Faculty of Engineering, King Mongkut's Institute of Technology Ladkrabang, Bangkok 10520, Thailand*
[2] *National Metal and Materials Technology Center, National Science and Technology Development Agency, Pathum Thani 12120, Thailand*
[3] *School of Engineering, Tokyo Institute of Technology, Tokyo 179-0085, Japan*

Received 12 October 2019
Revised 14 November 2019
Accepted 22 November 2019

ABSTRACT:
Diesel Engines are widely known for a high compression ratio, which is proportional to the engine's efficiency. The effect from direct injection of a diesel engine generates particulate matter (PM). PMs are mainly composed of Soot and Metallic Ash, which are harmful to human health. This research describes thermal efficiency, engine performance and combustion behavior at various load (20%, 50%, and 80%) and fuel (B7, B20, and B100) by using combustion pressure analyzer. The experimental results demonstrated that B100 has the highest ISFC and lowest ISEC for all test series owing to the highest indicated thermal efficiencies. Operating load and fuel are strongly proportional to heat release rate and ignition delay. The heat release rate of low load condition is retarded compare with medium and high load. Conventional diesel and biodiesel PMs were investigated by using Scanning electron microscopy (SEM) and Transmission electron microscopy (TEM). The average size of ultrafine particles that obtained from the experiment are range of 50-500 nm and primary nanoparticle size of B7 and B100 are in range of 25-50 nm.

Keywords: *Biodiesel, Compression Ignition Engine, Combustion Behavior, Particle Emission*

1. INTRODUCTION

Nowadays, the problems that have been taken seriously are the depletion of fossil fuel and global warming [1]. Many researchers try to replace conventional engine by electric vehicle and fuel-cell, but due to cost, driving distance, durability and some of engine's characteristics, it is difficult to overcome the conventional engine [2]. Owing to a high compression ratio, compression ignition (CI) engines or can be called Diesel engines are recognized as one of the highest thermal efficiency engines among internal combustion engines (ICE) [3]. Unfortunately, the usage of CI engine also releases two critical issues from exhaust gas which are particulate matter (PM) and nitrogen oxide (NO_x). Diesel particulate matters consist of soluble organic fraction (SOF) and solid fraction (metallic ash) as a main component [4]. The effects of these pollutant need to be prevented because they are harmful to human health, especially cancer. Thus, in order to decrease these variables an alternative fuel such as biodiesel has been chosen to be investigated in a small CI engine. Biodiesel has been frequently discussed as an alternative fuel to replace diesel owing to lower cost and particle emission. Moreover, it can conveniently obtain from renewable resources (Algae, Palm, Jatropha, Coconut etc.) [5-8]. Since it has a similar physical property to diesel fuel, the engine doesn't need to modify. This paper is aimed to investigate the engine's performance, combustion characteristics, particle emission and soot morphology of small diesel engine at various load (20%, 50% and 80%) and fuel (B7, B20 and B50), by

* Corresponding author: P. Karin
E-mail address: kkpreech@staff.kmitl.ac.th

using engine combustion analysis, heat release rate analysis, opacity smoke meter, scanning electron microscopy (SEM) and transmission electron microscopy (TEM).

2. METHODOLOGY

It can be seen from Table 1 that the Cetane Number (CN) of neat biodiesel (B100) is 27.27% higher than diesel (B7). CN is one of the most important properties as it mainly effects on an ignition delay and combustion duration. Moreover, kinematic viscosity of biodiesel is 50% higher than diesel, the disadvantages of higher viscosity are increasing loss (pumping energy in fuel line) and narrowing spray pattern [9]. High heating value (HHV) or calorific value (CV) of diesel is 18.33% higher than biodiesel due to higher percent carbon and hydrogen composition in a chemical formula. Distillation of diesel is lower than biodiesel, the main reason is because of diesel can vaporize easier than biodiesel owing to the smaller molecule [10].

3. EXPERIMENTAL SETUP AND CONDITION

Table 2 shows an engine specification of a single cylinder diesel engine (Kubota RT140 DI Plus ES) with unmodified fuel injection (fuel is injected at 19° C.A. Before Top Dead Center-BTDC with mechanical fuel injection system), rated power of 9.2 kW at 2,400 rpm, displacement volume of 709 cm^3 and compression ratio of 18:1 was coupled with eddy current dynamometer (Tokyo Plant Model ED-60-LC). In addition, a necessary instruments such as pressure sensor (Kistler 6052C31, 250 bar, sensitivity: ±0.5%), load cell, crank encoder (CA-RIE-360, resolution: 360 pulses/rev.), opacity smoke meter (OKUDA DSM-240), computer software (DAQ DEWEsoft SIRIUSi-HS-CA) and control system are required in order to analyze the parameters inside the combustion chamber.

Table 1: Fuel Properties.

Properties	Standard	Diesel (B7)	Biodiesel (B100)
Density (kg/m^3)	ASTM D4052	844.78	864.4
Cetane Number	ASTM D613	55	70
Kinematic Viscosity at 40 °C (mm^2/s)	ASTM D445	3.092	4.5
Chemical Formula		$C_{16.17}H_{32.00}$	$C_{15.26}H_{29.48}O_{1.70}$
Carbon Fraction	ASTM D5291	82	78
Bulk Modulus (MPa)		1,282	1,482
Flash Point (°C)	ASTM D93	65	184.5
Calorific Values (kJ/kg)	ASTM D240	46,800	39,550
Distillation (°C)			
T10	ASTM D86-11b	214.3	336.2
T30	ASTM D86-11b	250.3	339.7
T50	ASTM D86-11b	281.5	341.4
T70	ASTM D86-11b	312.5	345.4
T90	ASTM D86-11b	352.3	351.2

Table 2: Engine Specification.

Items	Details
Engine type	1-cylinder, Direct injection, Compression ignition
Bore x Stroke	97 mm x 96 mm
Displacement	$709cm^3$
Compression ratio	18:01
Rated power	9.2kW @ 2,400rpm
Injection timing	19° C.A. BTDC
Injection pressure	22MPa

Prior to the experiment, B7 as a substrate was blended with 20% of B100 by volume and become B20 (80% of diesel and 20% of biodiesel). At the first stage of this work, 2 groups of experiment tests (1) different engine's load (20%, 50% and 80%), and (2) different fuel (B7, B20 and B100), were performed. For comparability, all tests series were conducted at constant engine speed (2,400 rpm). The main focuses of this experiment are engine's performance, combustion characteristics and particulate matter.

3. RESULTS AND DISCUSSIONS

3.1 Engine performance

The engine performance parameters were included of indicated thermal efficiency (%), indicated specific fuel consumption (ISFC in unit of kg/kWh), and indicated specific energy consumption (ISEC in unit of kJ/kWh). In case of constant heating value, ISFC (amount of fuel utilized to provide a unit of engine power) and ISEC (amount of energy to provide a unit of engine power) of each condition could be the same. Figure 1 displays a pressure-volume diagram (P-V diagram) and pressure rise inside the combustion chamber versus crank angle degree (CAD) from -60 CAD to 60 CAD of B7, B20 and B100 at 20%, 50% and 80% load, respectively. The areas enclosed by the pressure curve were used to determine indicated work of the system. In case of B7 and B20 at 20% and 50 % loads, maximum pressure is similarly occurred at 5 CAD, whereas it can be observed that B100 at 50% load and all fuel at 80% load are retarded to 7 and 9 CAD respectively. This is mainly due to shorter ignition delay (IGD) and advancement of heat release rate (HRR).

ISFC and ISEC of all fuel show a declination when the engine is operated at higher load because of higher indicated thermal efficiency, as shown in Fig. 2. ISFC of B20 is 0.66% higher than B7 at 20% and 50% load, however at 80% load condition, B20 is consumed 6.61% fuel higher than B7 because of lower heating value. Moreover, B100 shows approximately 12.35% higher ISFC for all testing conditions. B100 presents approximately 4.01% lower ISEC for all load conditions, this is mainly due to the highest amount of oxygen content in a molecule which help to promote more complete combustion in a combustion chamber, thus it leads to the highest indicated thermal efficiency for every testing series. In addition, B20 shows 1.37% lower energy consumption than B7 in both 20% and 50% load, however, B20 consumes 4.46% higher energy consumption than B7 at 80% load.

3.2 Combustion characteristics

The combustion characteristics were included maximum heat release rate (MaxHRR in a unit of J/deg), maximum cumulative heat release (MaxCHR in a unit of J) and ignition delay. Heat release rate was calculated according to first law of thermodynamics [11]. There is a time delay (ignition delay) in between start of injection (SOI) and start of combustion (SOC). Figure 3 shows the effect of various fuel and same load testing series at 20%,50% and 80% on heat release rate. The positive region indicates the amount of energy release vice versa, the negative region of heat release rate indicates the total amount of energy that has been absorbed to change phase from liquid to gas. Moreover, maximum heat release rate is increased from 20% to 50% load, however, compare with 50% load, heat release rate of 80% load is decreased by approximately 6.2%. In addition, ignition delay is decreased from low to high load, respectively.

Table 3 presents quantitative information on same load and difference testing fuel conditions. The maximum pressure (MaxP. in a unit of bar) of every fuel on the same load testing are not significantly difference, whereas when the engine's load was increased from 20% to 80 % the maximum pressure also increased from 60 to 70 bar. B7 and B20 show the similar trend however B100 shows the lowest heat release rate and most advance ignition delay among all others fuel owing to largest molecular structure, poorest vaporization, highest viscosity and highest cetane number. In addition, the greater Bulk Modulus of biodiesel leads to an advancement in fuel injection timing [12, 13].

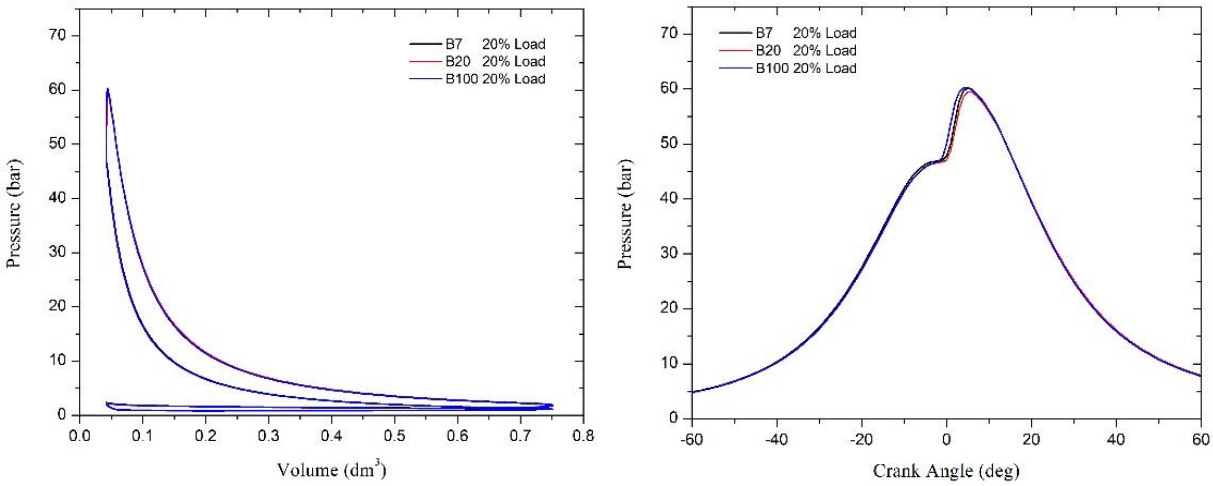

(a) 20% load

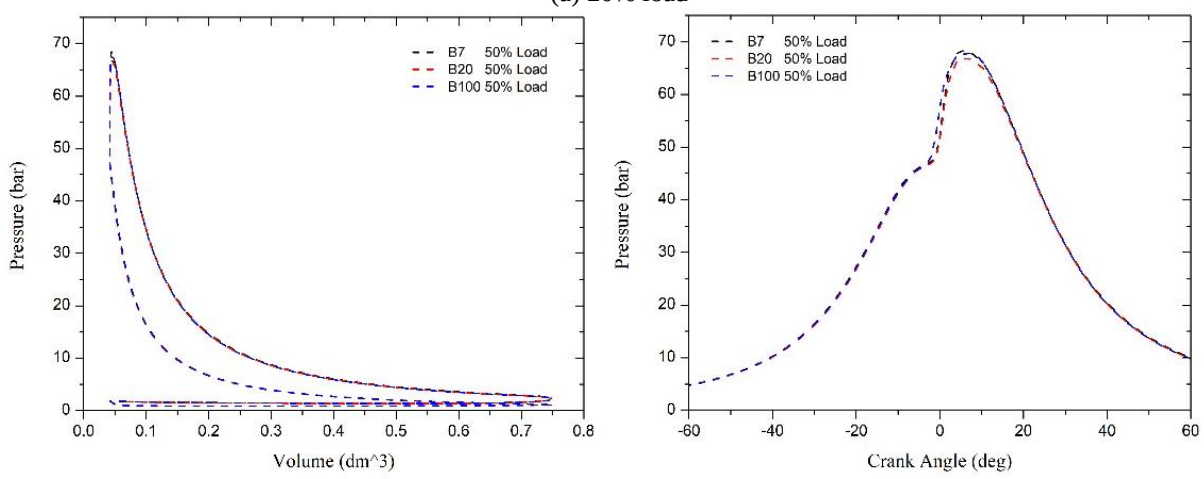

(b) 50% load

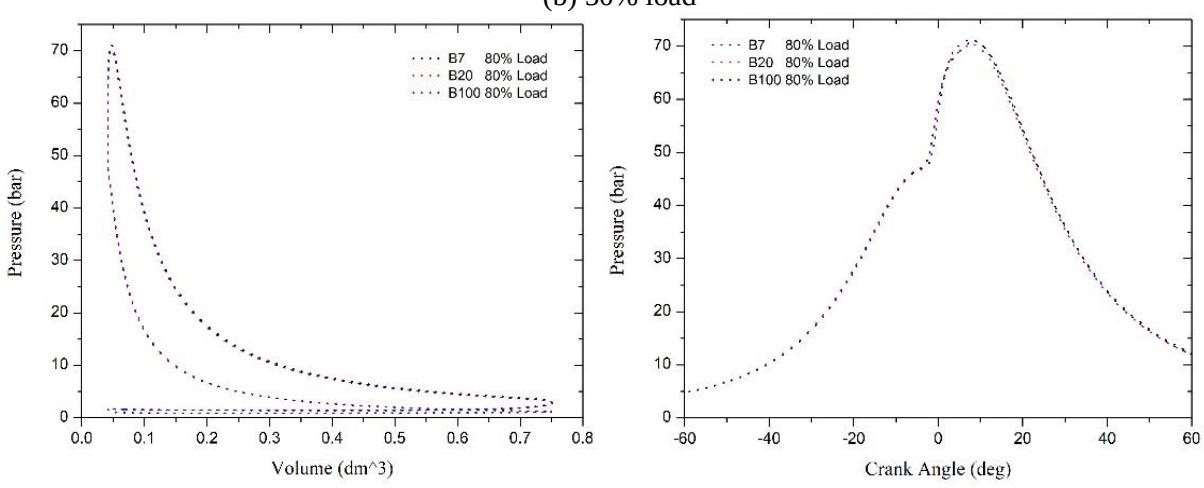

(c) 80% load

Fig. 1. P-V and P-θ diagrams in the condition of constant engine speed of 2400 rpm and load of (a) 20%, (b) 50% and (c) 80% with various fuel.

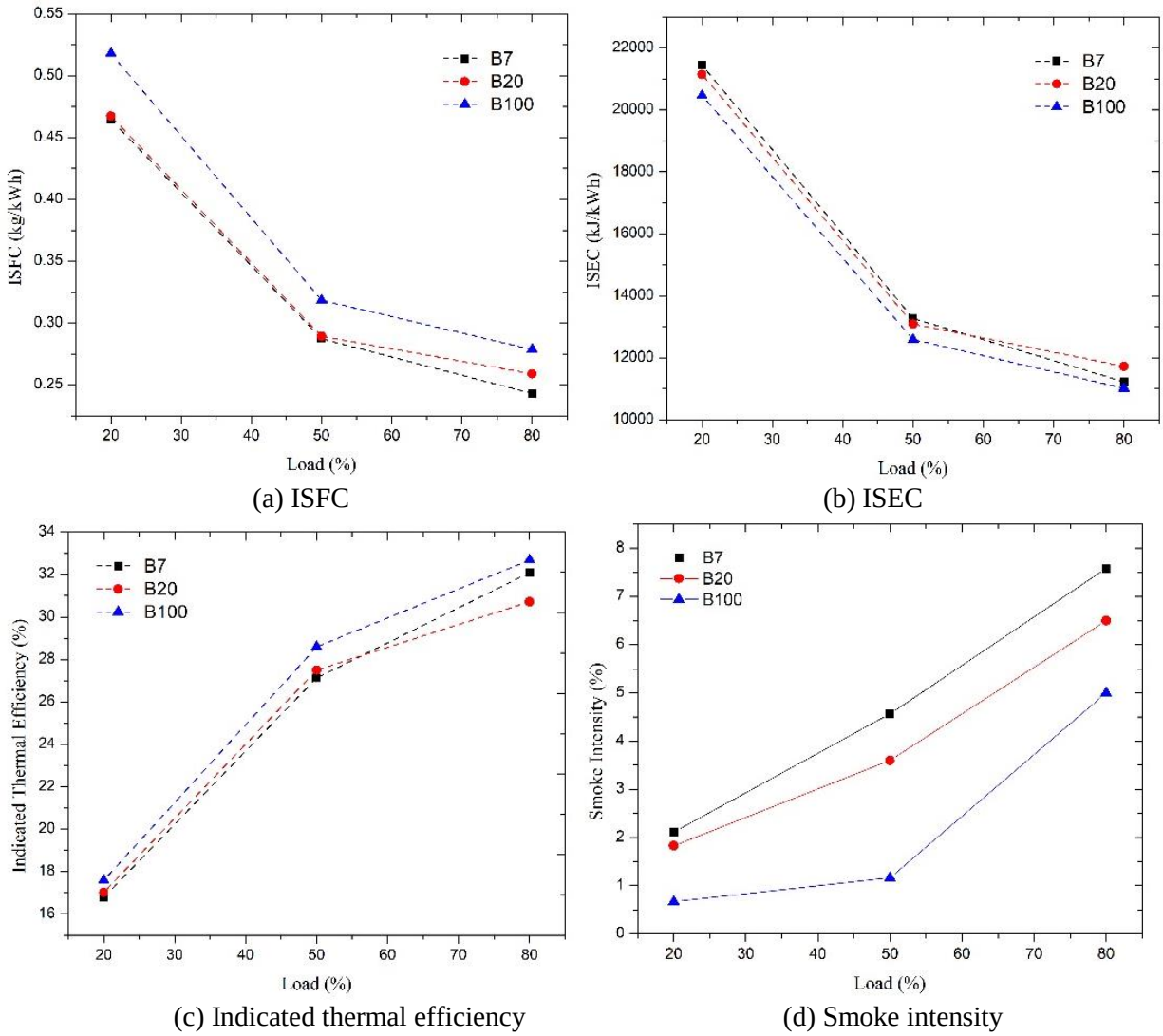

Fig. 2. Comparison of (a) indicated specific fuel consumption, (b) indicated specific energy consumption, (c) indicated thermal efficiency and (d) smoke intensity at the constant engine speed of 2400 rpm, various load and fuel.

Table 3: Quantitative information based on same load and difference fuel.

	20% Load			**50% Load**			**80% Load**		
Fuel	**B7**	**B20**	**B100**	**B7**	**B20**	**B100**	**B7**	**B20**	**B100**
MaxP. (bar)	60	59	60	69	67	68	71	70	71
MaxP.CAD. (deg)	5	5	5	5	5	7	7	9	9
MaxHRR (J/deg)	47	46	42	68	64	56	60	57	50
MaxHRR.CAD. (deg)	2	3	1	1	1	0	0	-1	-1
MaxCHR (J)	353	356	343	616	602	595	891	849	860
IGD (ms)	1.46	1.46	1.39	1.39	1.39	1.32	1.32	1.25	1.25

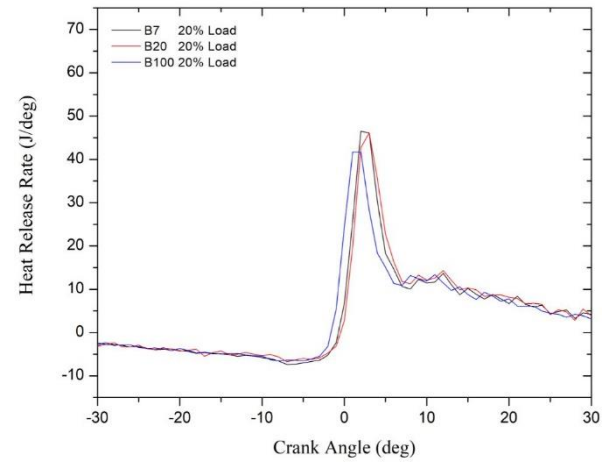

(a) 20% load

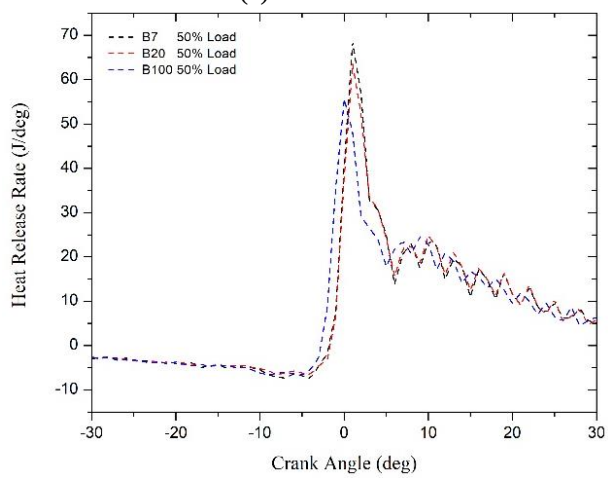

(b) 50% load

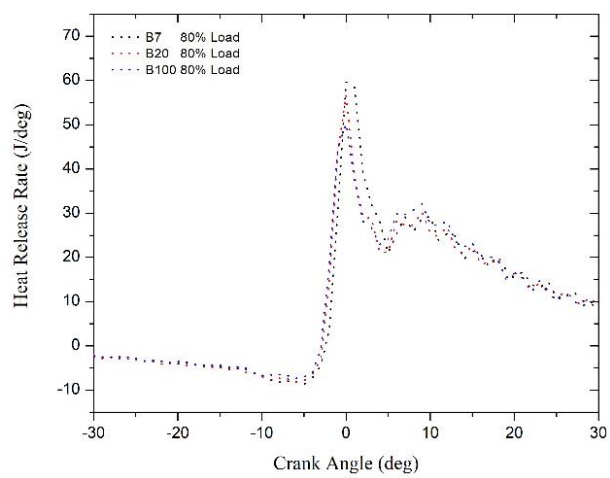

(c) 80% load

Fig. 3. Heat release rate in the condition of constant engine speed of 2400 rpm and load of (a) 20%, (b) 50% and (c) 80% with various fuel.

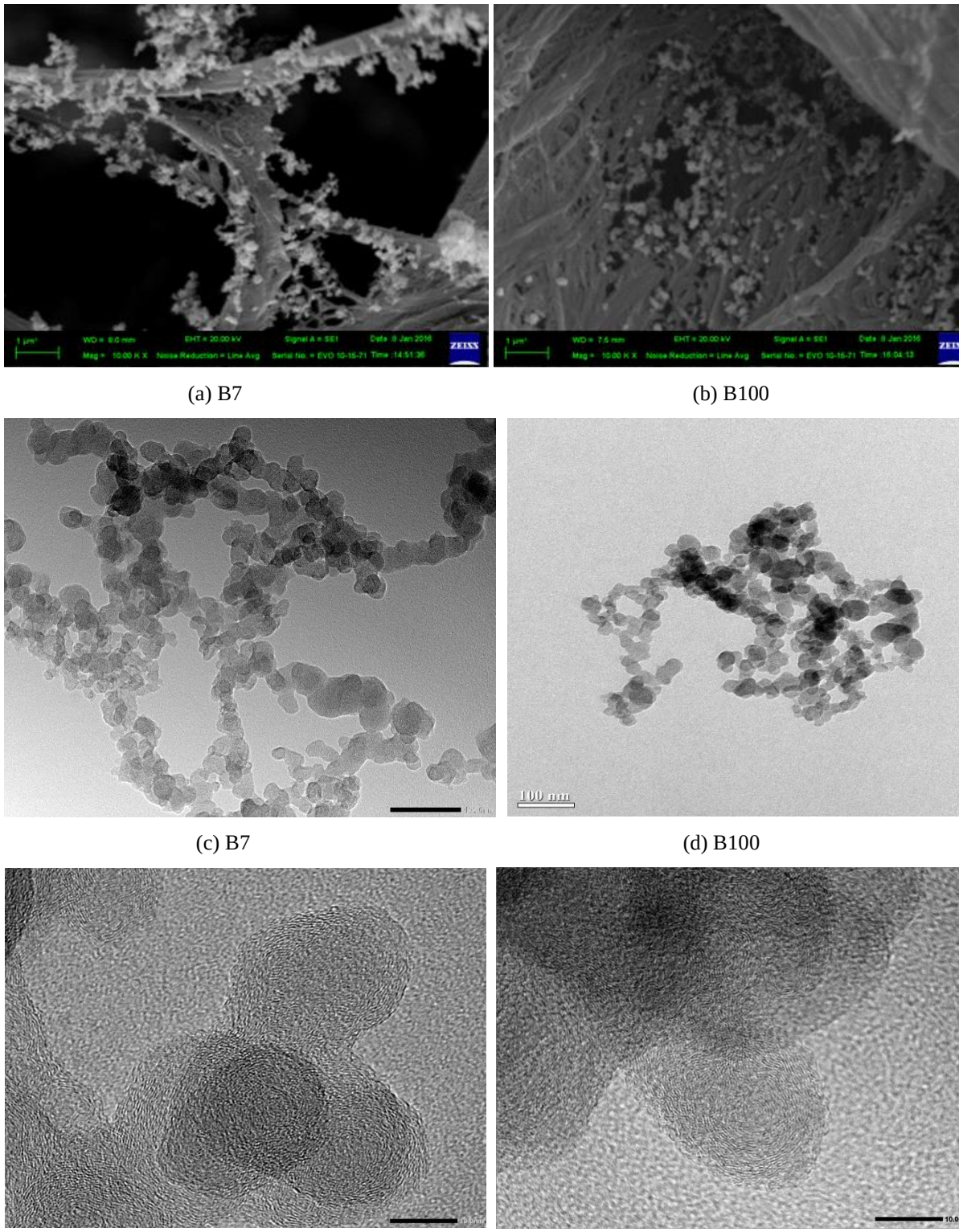

(a) B7 (b) B100

(c) B7 (d) B100

(e) B7 (f) B100

Fig. 4. SEM images of aggomerated soots of (a) B7 and (b) B100, TEM images of aggregated ultrafine soot of (c) B7 and (d) B100, TEM images of soot primary nanoparticle of (e) B7 and (f) B100.

3.3 Particulate matter and soot morphology

Smoke intensity of each fuel versus engine loads at 2,400 rpm was measured by opacity smoke meter. As a consequence of highest oxygen content and highest indicated thermal efficiency, B100 has the lowest smoke intensity in all load conditions (see Figure 2d.). The reduction of soot could reduce the radiation heat loss from the engine [14]. Conventional diesel (B7) and B20 have significantly higher smoke intensity compare with B100, especially at 50% load. The smoke intensity is an in direct method to figure out the quantity of PM's in a large scale via the paper filter. Moreover, the amount of fuel injected into the combustion chamber is directly proportional to engine load and smoke intensity.

Particulate matter from engine combustion can be characterized into 2 main groups as volatile and non-volatile matter. Soot and ash which can be considered as a non-volatile matters are generated from incomplete combustion of fuel in a combustion chamber, while others non-volatile matters (such as metallic ash) come from in purity of air, lubricant oil and material break down inside the engine (such as wear scar and abrasive).

The nanostructure and morphology of the PMs were investigated by using both SEM and TEM. The size of diesel engine's PMs are described as PM10 (For diameter (D) < 10 μm), fine particles (D < 2.5 μm), ultrafine particles (D < 100 nm) and nanoparticles (D < 50 nm) [15]. Figure 4 shows SEM images of agglomerate fine particles of B7, and B100. In addition, TEM images of agglomerated ultrafine particles of B7 and B100 can also clearly observed. The average agglomerated of ultrafine particles size are in range of 50-500 nm [16]. The oxygenated fuel is strongly promoted more complete combustion thus the agglomerated of ultrafine particle of PMs gradually reduce from B7 to B100. The primary soot nanoparticles are separated into two main part as an inner core and outer shell [17, 18]. Moreover, primary nanoparticles size of B7 and B100 are in range of 25-50 nm. From morphology point of view, the nanoparticles size of conventional diesel and biodiesel are not significantly different.

4. CONCLUSION

Through the experiment of engine test with different load (20%, 50% and 80%) and fuel (B7, B20 and B100) in a small compression ignition engine. As a result of engine performance, maximum pressure of varying fuel on the same load condition are similar. However, at the high load condition, maximum pressure is retarded. B100 shows the highest fuel consumption per unit of engine power in every testing condition, nevertheless as a consequence of lowest heating value and highest indicated thermal efficiency, B100 shows the lowest energy consumption per unit of engine power. Moreover, from the combustion characteristic, ignition delay could be reduced by either increase the proportion of biodiesel or increase the engine's load. B100 shows the shortest ignition delay and lowest heat release rate at the same load condition, owing to largest molecular structure, poorest vaporization, highest viscosity and highest cetane number. In addition, the greater Bulk Modulus of biodiesel leads to an advancement in fuel injection timing. The smoke intensity of B100, B20 and B7 is increased ascending, because of amount of oxygen contents in a molecule. In the same manner, agglomerated ultrafine particles size of PMs gradually reduce from B7 to B100, however, nanoparticles size of conventional diesel and biodiesel are not significantly different.

ACKNOWLEDGEMENTS

The authors gratefully acknowledge the financial and facilities support from Thailand Research Fund, National Science and Technology Development Agency and Bangchak Corporation Public Company Limited.

REFERENCES

[1] Höök, M. and Tang, X. Depletion of fossil fuels and anthropogenic climate change, A review Energy Policy, Vol. 52, 2013, pp. 797-809.
[2] Gelmanova, Z.S., Zhabalova, G.G., Sivyakova, G.A. and Lelikova, O.N. Electric cars advantages and disadvantages, IOP Conf. Series: Journal of Physics: Conf. Series, Vol. 1015, 2018, pp. 1-6.
[3] Zheng, J.J., Wang, J.H., Wang, B. and Huang, Z.H. Effect of the compression ratio on the performance and combustion of a natural-gas direct-injection engine, Proceedings of the Institution of Mechanical Engineers, Part D: Journal of Automobile Engineering, Vol. 223(1), 2009, pp. 85-98.

[4] Karin, P., Watanawongskorn, P., Boonsakda, J., Saenkhumvong, E., Rungsritanapaisan, S., Srivarocha, S., et al. Impact of biodiesel on small CI engine combustion behavior and particle emission characteristics, SAE. Int. Conf., 2017-32-0094, 2017, pp. 1-8.
[5] Ihsanullah, Shah, S., Ayaz, M., Ahmed, I., Ali, M., Ahmad, N., et al. Production of biodiesel from algae, Journal of pure and applied microbiology, Vol. 9(1), 2015, pp. 79-85.
[6] Zahan, K.A. and Kano, M. Review of biodiesel production from palm oil, Energies, Vol. 11(8), 2018, pp. 1-25.
[7] Liaquat, A.M., Masjuki, H.H., Kalam, M.A., Rizwanul Fattah, I.M., Hazrat, M.A., Varman, M., et al. Effect of coconut biodiesel blended fuels on engine performance and emission characteristics, Procedia Engineering, Vol. 56, 2013, pp. 583-590.
[8] Hoekman, S.K., Broch, A., Robbins, C., Ceniceros, E. and Natarajan, M. Review of biodiesel composition, properties, and specifications, Renewable and Sustainable Energy, Vol. 16(1), 2012, pp. 143-169.
[9] Karmakar, A., Karmakar, S. and Mukherjee, S. Properties of various plants and animals feedstocks for biodiesel production, Bioresource Technology, Vol. 101(19), 2010, pp. 7201-7210.
[10] Watanawongskorn, P., Karin, P., Charoenphonphanich, C., Boonsakda, J., Hanamura, K., and Chollacoop N. Impact of diesel engine combustion characteristics on particulate Matter's morphology and nanostructure from ethanol-blended biodiesel, paper presented in the JSAE International Conference, 2017, Yokohama, Japan.
[11] Heywood, J.B. Internal combustion engine fundamentals, 2nd edition, 1988, McGraw-Hill, New York.
[12] Boehman, A.L., Morris, D., Szybist, J. and Esen, E. The impact of the bulk modulus of diesel fuels on fuel injection timing, Energy Fuels, Vol. 18(6), 2004, pp. 1877-1882.
[13] Szybist, J.. and Boehman, A. Behavior of a diesel injection system with biodiesel fuel, SAE Technical Paper Series, 2003-01-1039, 2003, pp. 1-11.
[14] Bertrand, P.A.M. Soot formation of lignin derived fuels in a laminar co-flow diffusion flame, Thesis, Technics University Eindhoven, Department of Mechanical Engineering, Section Combustion Technology, Eindhoven, Netherlands, 2009.
[15] Kittelson, D.B. Engines and nanoparticles, Journal of Aerosol Science, Vol. 29(5-6), 1998, pp. 575-588.
[16] Karin, P., Songsaengchan, Y., Laosuwan, S., Charoenphonphanich, C., Chollacoop, N. and Hanamura, K. Nanostructure investigation of particle emission by using TEM image processing method, Energy Procedia, Vol. 34, 2013, pp. 757-766.
[17] Ishiguro, T., Takatori, Y. and Akihama, K. Microstructure of diesel soot particles probed by electron microscopy: First observation of inner core and outer shell, Combustion and Flame, Vol. 108(1), 1997, pp. 231-234.
[18] Karin, P., Boonsakda, J., Siricholathum, K., Saenkhumvong, E., Charoenphonphanich, C. and Hanamura, K., Morphology and oxidation kinetics of CI engine's biodiesel particulate matters on cordierite Diesel Particulate Filters using TGA, International Journal of Automotive Technology, Vol. 18(1), 2017 pp. 31-40.